Journal of Machine Engineering, 2024, Vol. 24, No. 1, 87–102
ISSN 1895-7595 (Print) ISSN 2391-8071 (Online)

Received: *05 January 2024* / Accepted*: 28 February 2024* / Published online: *12 March 2024*

plastic deformation, clad layer, restoration, creep theory

Huy-Tuan PHAM[1], Gulmira Zhaibergenovna BULEKBAYEVA[2], Abzal Uteuovich TABYLOV[2], Amina Zakharovna BUKAYEVA[2*], Nabat Bazarkhanovna SUIEUOVA[2], Asgerbek Alievich YUSUPOV[2], Gulmira Smagulovna BILASHOVA[2], Gulsara Sapiyevna MAMBETALIYEVA[2]

ANALYSIS OF ONE-DIMENSIONAL INELASTIC DEFORMATION OF THE CLAD LAYER BY ROLLING FOR RESTORATION OF FLAT SURFACE PARTS

The hardening-finishing treatment of parts surface with rolling by steel cylindrical rollers produces low roughness, reduced residual compression stresses, and fine-grained structure due to plastic deformations. The deformation of metals during machining at high temperatures is characterized by a significant influence of strain rates on stresses. This necessitates the calculation of stresses and strains based on the equation of state of rheonic bodies. This study aims to determine the components of stresses and force factors of the technological process of finishing and strengthening machining of the surface of parts by deriving the analytical solutions to calculate the stress-strain state within the deformation zone based on creep theory. In this problem, general formulas are obtained for calculating the stress-strain state, pressure and friction forces on the contact surface, as well as forces and moments acting on the roller. Numerical analysis using Mathcad explores the understanding of the stress-strain state in the deformation zone on the force factors of the technological process. The obtained results are beneficial for establishing the mode of thermomechanical processing and selecting appropriate technological equipment for restoring flat surface parts.

1. INTRODUCTION

One effective way of hardening the surface layer of the part, increasing its wear resistance, and achieving high accuracy is the process of surface deformation by the rolling method, which consists of changing its geometric, physical, and mechanical parameters [1–2]. Several studies have been carried out to improve the quality of the working surfaces of parts instead of using the traditional thermal methods. The running-in of working surfaces of parts by surface-plastic deformation provides low roughness by deposition of metal in thickness in the seam area to create plastic tensile strains in the longitudinal and transverse directions and residual compressive stresses in the surface layers with the formation of fine

[1] Faculty of Mechanical Engineering, Ho Chi Minh City University of Technology and Education, Vietnam
[2] Department of Mechanical Engineering and Transport, Caspian University of Technologies and Engineering named after Sh. Yessenov, Kazakhstan
[*] E-mail: amina_bukaeva@mail.ru
https://doi.org/10.36897/jme/185475

grain structure [3–5]. This process is realized due to metal deposition by cylindrical rollers along the thickness in the weld zone to induce plastic elongation deformations.

Tonysheva and others [6] determined the parameters characterizing the technological process of rolling, including the rolling force on the roller, the radius and width of the roller, the thickness of the metal in the rolling zone, and the parameters of the material state. They found that residual deformations are eliminated if the plastic elongation deformations are created by rolling in the layer and adjacent to the seam. In this case, the longitudinal residual stresses are close to zero. Together with the elimination of longitudinal residual deformations, the running-in process eliminates the displacement of the structure resulting from the loss of stability due to the action of longitudinal residual stresses. The proposed impact parameters are calculated by approximate formulas according to the scheme of uniaxial stress state [7]. At the same time, the condition of settling the running-in zone in the form of specified deformations along the thickness of the element is accepted.

For an objective analysis of the effect of deposition through the thickness of the heated material, and assessment of changes in residual stresses and deformations, it is required to perform a study of the stress-strain state of the layered metal, based on which the deforming force and total power are additionally calculated [8]. As noted, as the temperature increases, it is reasonable to calculate technological processes of metal processing based on the equations of state of the simplest creep theories. The most general in this respect is the theory of hardening. In the considered case, in contrast to the usual rolling process between rotating drive rolls, the deforming roller makes plane-parallel movement, and there are different friction conditions on the contact surfaces. In the works of Sergeev, Karamyshev and others, experimental data showed that the deformation of metals during processing at high temperatures is characterized by a significant influence of strain rates on stresses [9, 10]. Therefore, it is necessary to calculate stresses and strains based on the equation of state of rheonic bodies.

The creep theory establishes the relation between stresses, strains, rates of their change, and time in the simplest case of uniaxial stretching. It presents the possibility of describing the deformation of a material in the general case of time-varying stresses and strains based on the simplest tests of the material. It provides the determination of the law of strain variation by a given law of stress variation and vice versa. In a particular case, it should allow the construction of relaxation curves from a series of creep curves. The simplest but not the best method of verifying the creep theory is to compare the results of the experimental study of relaxation at constant strain with the data obtained from the creep theory.

2. METHODOLOGY

Considering the simplest creep theories to describe the creep processes of metals, applying these to the problems of metal processing allows us to obtain reliable results with less effort and time. It should be noted that the simplest theories consider the main variables: strain rate, stress, and time. After selecting the variables, it is necessary to link them with a particular analytical relationship that is adequately consistent with the data of experimental experiments. Creep theory construction is usually performed for the simplest case of uniaxial stretching and the general case of nonuniaxial stress state [8–10].

The stress, creep strain and creep strain rate are taken as the main variables in the theory of hardening. It is assumed that at a given temperature there is a certain dependence between these variables:

$$\Phi_3(\varepsilon_c, \sigma, \xi_c) = 0 \tag{1}$$

Usually this equation is taken in the form

$$\xi_c \varepsilon_c^{\beta} = f(\sigma) \tag{2}$$

Since:

$$f(\sigma) = \alpha\sigma^{\nu} \tag{3}$$

Equation (2) will be written as follows:

$$\xi_c \varepsilon_c^{\beta} = \alpha\sigma^{\nu} \tag{4}$$

where: α, β, ν – temperature-dependent material constants.

After integration of equation (4) at $t = 0$, $\xi_c = 0$ we find

$$\varepsilon_c = [(\beta + 1)\alpha\sigma^{\nu} t]^{\frac{1}{\beta+1}} \tag{5}$$

Then the equation describing the creep curves according to the theory of hardening has the form:

$$\varepsilon = \varepsilon_l + \varepsilon_c = \frac{\sigma}{E} + [(\beta + 1)\alpha\sigma^{\nu} t]^{\frac{1}{\beta+1}} \tag{6}$$

It follows from the equation that the creep curves in this case are geometrically similar. From equation (6) by integration at $t = 0$, $\sigma = \sigma(0)$ we obtain:

$$t = \frac{1}{\alpha E^{\beta+1}} \int_{\sigma}^{\sigma(0)} \frac{[\sigma(0) - \sigma]^{\beta}}{\sigma^{\nu}} d\sigma \tag{7}$$

Equation 7 describes the family of relaxation curves in implicit form. For arbitrary values of ν and β, the integral (7) is determined numerically.

For an uniaxial stress state, the equation (4) has the following form

$$\sigma_e = a\xi_e^m \kappa^n \tag{8}$$

where: $\kappa = \int \xi_e \, dt$ - Udquist parameter, σ_e - equivalent stress, ξ_e - equivalent strain rate.

As a special case, the nonlinear viscous equation, widely used in the analysis of flow in superplasticity state, follows from the hardening theory:

$$\xi_e = K\sigma_e^{\nu} \tag{9}$$

where: K, ν – material constants at a certain temperature

For uniaxial stress state equation (9) has the form:

$$\xi = K\sigma^{\nu} \tag{10}$$

From equation (8), as a special case (at m = 0), we obtain the equation used to study the deformation of purely plastic materials, including perfectly rigid plastic material (at $m = 0, n = 0$).

For numerical calculations of the stress-strain state of the layer in the deformation zone, it is necessary to know the values of the material constants at the temperature of shape change. The material constants (parameters of the equation of state) are determined by processing creep curves. Equation of state (4) describes creep curves with an explicit hardening section (first section) and equation of state (10) describes creep curves with no hardening section and an explicit steady-state creep section (second section).

Methods for determining the parameters of the equation of state are given in [11–14]. The degree of coincidence of experimental and theoretical creep curves depends on the accuracy of determining the parameters of the equation of state (material constants). Reliability of calculation of stress-strain state and force parameters of technological process depends on the accuracy of material constants.

3. RESULTS AND DISCUSSIONS

Consider the deformation of the material under the action of a rigid cylindrical roller, which performs a plane-parallel motion in the plane of the drawing (Fig. 1). The deformable material is located on a rigid surface. Denote the speed of movement of the center of the roller by V_0 and the angular velocity of rotation ω; it is believed that they are constant values in time. The movement velocity components of an arbitrary point on the contact surface of the material with the roller in the deformation focus are illustrated in Fig. 1.

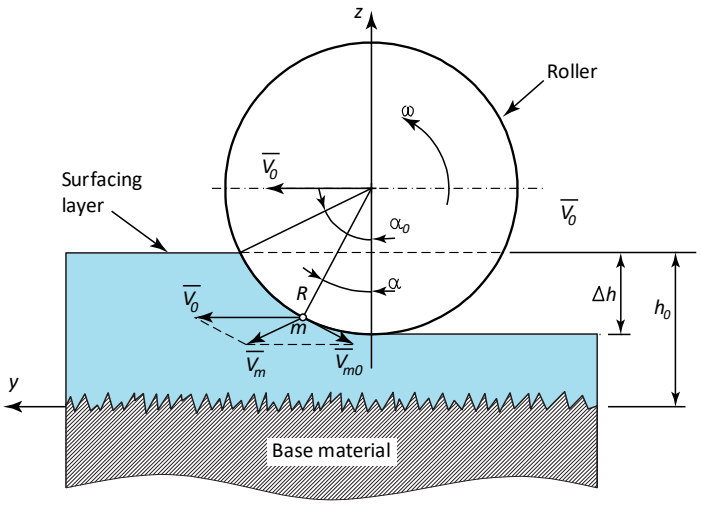

Fig. 1. Cylindrical roller running-in scheme

where: R- roller radius, Δh - changing the layer thickness, h_0- thickness of the rolled layer, α_0 − maximum contact angle, α - angular coordinate of the point m, ω - angular rotation

speed of the roller, $\bar{V}_0$ – velocity vector of movement the center of the roller, $\overline{V_m}$- the velocity vector of the point m on the contact surface, $\bar{V}_{m0}$- the vector of the rotation speed of the point m relative to the center of the roller.

$$v_y = v_0 - \omega R \cos\alpha \tag{11a}$$

$$v_z = -\omega R \sin\alpha \tag{11b}$$

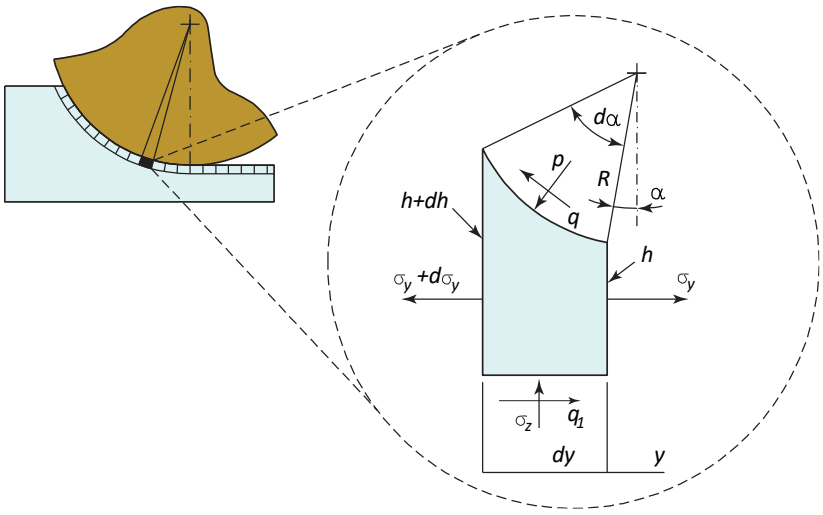

Fig. 2. Derivation of the equilibrium equation of a finite element

Suppose that the stress-strain state of the material changes only along the y coordinate. Then, from the equilibrium condition of a finite element of the body, we have the following equations (Fig. 2):

$$\frac{d\sigma_y}{dy} + \frac{\sigma_y + p}{h} tg\alpha + \frac{q - q_1}{h} = 0 \tag{12}$$

$$\sigma_z = p - qtg\alpha \tag{13}$$

where σ_y, σ_z, p, q are stress components, the pressure and intensity of the friction forces, respectively, on the contact surface of the material with the roller; q_1 is the intensity of the friction forces of a material with a rigid surface.

In technological problems of this kind in a one-dimensional formulation, the equivalent stress σ_e is approximately calculated as [6]:

$$\sigma_e = \sigma_y - \sigma_z \tag{14}$$

It is obvious from Fig. 2 that $h = h_0 + R(1 - \cos\alpha)$, $dy = R\cos\alpha\, d\alpha$. Considering the relations in equations (12)-(14), after simple transformations, an ordinary differential equation is obtained:

$$\frac{d\sigma_y}{d\alpha} + \psi_1(\alpha)\sigma_y = \psi_2(\alpha) \tag{15}$$

The following section analyses the stress-strain state of the layer and force parameters of the technological process. To integrate equation (15), we have the boundary condition $\alpha = 0,\ \sigma_y = 0$. Then, the solution of the equation will be written as follows:

$$\sigma_y = exp\left(-\int_0^\alpha \psi_1 d\alpha\right)\int_0^\alpha \psi_2\, exp\left(\int_0^\alpha \psi_1 d\alpha\right) d\alpha \tag{16}$$

For small contact angles, the solution of the differential equation (15) has the form:

$$\sigma_y = \frac{1}{\lambda} exp\left(-\frac{\mu\alpha}{\lambda}\right)\left[(1+\mu^2)\int_0^\alpha \sigma_e\, exp\left(\frac{\mu\alpha}{\lambda}\right)\alpha d\alpha + \left(\frac{\chi}{2}+\mu\right)\int_0^\alpha \sigma_e\, exp\left(\frac{\mu\alpha}{\lambda}\right) d\alpha\right] \tag{17}$$

where $\lambda = h_0/R$ is the length carrying ratio.

As can be seen from the solutions obtained, in order to calculate the stresses, it is necessary to describe the state of the deformable material. Let's take the equation of state according to the theory of hardening in equation (8).

The rate of deformation in the longitudinal direction, taking into account the equations (11a,b), is calculated as:

$$\xi_y = \frac{dv_y}{dy} = \omega R\, sin\,\alpha \frac{d\alpha}{dy} \tag{18}$$

In the considered case of a plane deformed state [7, 8], the equivalent rate of deformations $\xi_e = 2\xi_y/\sqrt{3}$. Following Fig. 2, if we take into account that $d\alpha/dy = dl/(Rdy) = 1/(R\,cos\,\alpha)$, then for the strain rate and the equivalent strain rate we have:

$$\xi_y = \omega tg\alpha \tag{19a}$$

$$\xi_e = 2\omega tg\alpha/\sqrt{3} \tag{19b}$$

The Udquist parameter, taking into account the second equality (19) and the ratio $dt = d\alpha/\omega$, will take the form:

$$\kappa = -\frac{2}{\sqrt{3}} ln|cos\,\alpha| \tag{20}$$

If we take into account the formulas for the equivalent strain and the Udquist parameter in the equation (18), then to calculate the equivalent stress we obtain:

$$\sigma_e = a\left(\frac{2}{\sqrt{3}}\right)^{m+n} \omega^m tg^m\alpha(-ln|cos\,\alpha|)^n \tag{21}$$

From equation (13), taking into account equations (14) and (2), we determine the pressure distribution on the contact surface of the material with the roller:

$$p = \frac{\sigma_y - \sigma_e}{1 - \mu tg\alpha} \tag{22}$$

Taking into account the first equation (19), the deformation in the longitudinal direction is equal to:

$$\varepsilon_y = \int_0^t \xi_y dt + \varepsilon_y^0 = -ln|cos\,\alpha| + \varepsilon_y^0 \tag{23}$$

where ε_y^0 is the residual deformation after surfacing.

In order to completely eliminate the residual longitudinal deformations, it is necessary to fulfill the condition $ln|cos\,\alpha| = \varepsilon_y^0$. Appropriate contact angle:

$$\alpha_0 = arccos\left[exp\left(\varepsilon_y^0\right)\right] \tag{24}$$

On the other hand, the maximum contact angle (Fig. 1):

$$\alpha_0 = arcsin\left[2\sqrt{\Delta h/(2R)}\right]. \tag{25}$$

where Δh is the reduced thickness of the deposited layer.

Comparing equations (24) and (25), we find:

$$\Delta h = R\left[1 - exp\left(2\varepsilon_y^0\right)\right]/2 \tag{26}$$

If the magnitude of the residual longitudinal welding deformation is known, then formulas (24) and (26) determine the maximum contact angle of the material with the roller and the deformation $\varepsilon_z = \Delta h/h$ by the thickness of the element in the rolling zone of the weld seam [15, 16]. After determining the contact pressure and the intensity of the friction forces, the force and moment acting on the roller can be calculated.

The moment of forces per unit length in the direction perpendicular to the drawing, assuming that the moment of contact pressure forces relative to the center of the roller can be neglected, is equal to:

$$M = \mu R^2 \int_0^{\alpha_0} p d\alpha \tag{27}$$

Projection on the vertical and horizontal axis of the force per unit length in the direction perpendicular to the drawing, we obtained:

$$P_z = R\int_0^{\alpha_0} (p\,cos\,\alpha - q\,sin\,\alpha)d\alpha \tag{28}$$

$$P_y = R\int_0^{\alpha_0} (p\,sin\,\alpha + q\,cos\,\alpha)d\alpha \tag{29}$$

In the formulas obtained above, the integrals are calculated numerically. To do this, we introduce dimensionless quantities:

$$\bar{\sigma}_e = \frac{\sigma_e}{a\omega^m}, \quad \bar{\sigma}_{y,z} = \frac{\sigma_{y,z}}{a\omega^m}, \quad \bar{p} = \frac{p}{a\omega^m}, \quad \bar{M} = \frac{M}{a\omega^m R^2}, \quad \bar{P}_{y,z} = \frac{P_{y,z}}{a\omega^m R} \quad \bar{q} = \frac{q}{a\omega^m},$$

$$\bar{v}_{y,z} = \frac{v_{y,z}}{\omega R}, \qquad \overline{\psi_2}(\alpha) = \psi_2(\alpha)/(a\omega^m), \qquad \bar{\xi}_{e,y} = \frac{\xi_{e,y}}{\omega}, \qquad \overline{\Delta h} = \frac{\Delta h}{R}, \qquad \lambda = \frac{h_0}{R}$$

The above basic equations in dimensionless quantities will take the form:

$$\bar{\psi}_2(\alpha) = \frac{1}{\lambda + 1 - cos\,\alpha}\left(\frac{sin\,\alpha + \mu\,cos\,\alpha}{1 - \mu tg\alpha} + \frac{\chi}{2}cos\,\alpha\right)\bar{\sigma}_e \tag{30a}$$

$$\bar{\sigma}_y = exp\left(-\int_0^\alpha \psi_1 d\alpha\right)\int_0^\alpha \bar{\psi}_2\, exp\left(\int_0^\alpha \psi_1 d\alpha\right)d\alpha \tag{30b}$$

$$\bar{\sigma}_y = \frac{1}{\lambda} exp\left(-\frac{\mu\alpha}{\lambda}\right)\left[(1+\mu^2)\int_0^\alpha \bar{\sigma}_e\, exp\left(\frac{\mu\alpha}{\lambda}\right)\alpha d\alpha + \left(\frac{\chi}{2} + \mu\right)\int_0^\alpha \bar{\sigma}_e\, exp\left(\frac{\mu\alpha}{\lambda}\right)d\alpha\right] \tag{30c}$$

$$\bar{\xi}_y = tg\alpha \tag{30d}$$

$$\bar{\xi}_e = 2tg\alpha/\sqrt{3} \tag{30e}$$

$$\bar{p} = \frac{\bar{\sigma}_y - \bar{\sigma}_e}{1 - \mu tg\alpha} \tag{30f}$$

$$\bar{\sigma}_e = \left(\frac{2}{\sqrt{3}}\right)^{m+n} tg^m\alpha(-ln|cos\,\alpha|)^n \tag{30g}$$

$$\Delta\bar{h} = [1 - exp(2\varepsilon_y^0)]/2 \tag{30h}$$

$$\alpha_0 = arcsin\left[2\sqrt{\Delta\bar{h}/2}\right] \tag{30i}$$

$$\bar{M} = \mu\int_0^{\alpha_0} \bar{p} d\alpha \tag{30j}$$

$$\bar{P}_z = \int_0^{\alpha_0} (\bar{p}\,cos\,\alpha - \bar{q}\,sin\,\alpha)d\alpha \tag{30k}$$

$$\bar{P}_y = \int_0^{\alpha_0} (\bar{p}\,sin\,\alpha + \bar{q}\,cos\,\alpha)d\alpha \tag{30l}$$

Thus, in one-dimensional formulation, relatively general formulas for calculating the stress-strain state, pressure and friction forces on the contact surface, forces and moments acting on the roller were obtained. In order to perform the numerical calculation, a program in Mathcad system was compiled. The material deformation was calculated for the following values of constants: $m = 0.147; n = 0.157; \mu = 0.3; \chi = 1; \lambda = 0.1$. The value of residual deformation after cladding was taken $\varepsilon_y^0 = -8.7 \times 10^{-3}$; and $\Delta h/R = 8.7 \times 10^{-3}$ [17–20].

Figure 3 shows the distributions of dimensionless values of stress components (σ_y, σ_z) and equivalent stress (σ_e) in the deformation center. As can be seen from Fig. 3, the stresses are positive in the axial direction, so the residual tensile stresses after welding, will increase when the weld is run-in.

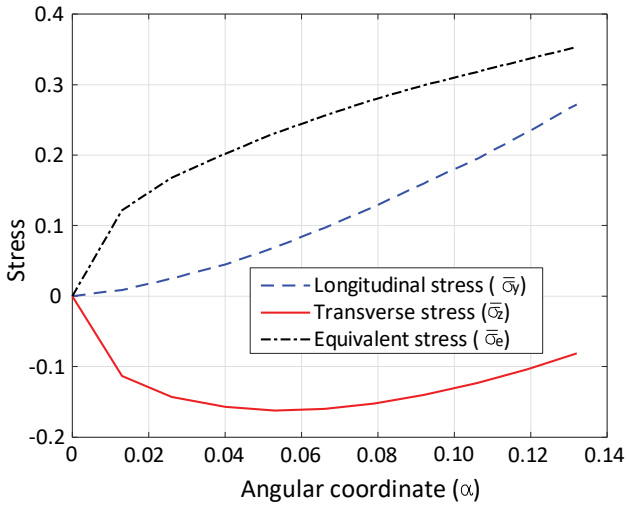

Fig. 3. Distribution of stress components and equivalent stress in the deformation center ($\mu = 0.3;\ \lambda = 0.1$)

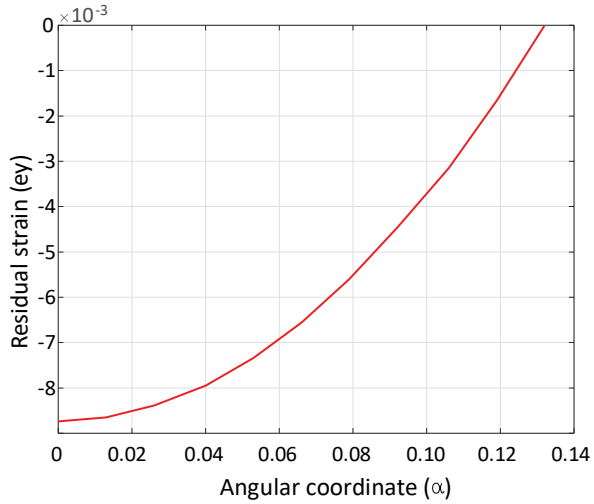

Fig. 4. Variation of residual strain in the axial direction of the layer

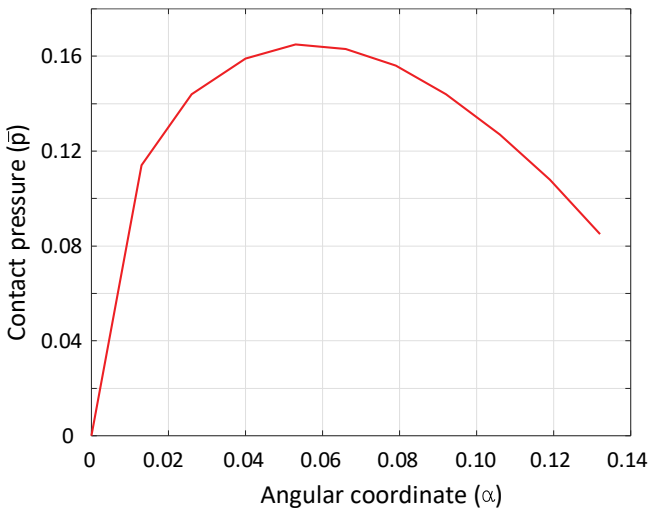

Fig. 5. Distribution of contact pressure on the roller

Figure 4 shows the variation of residual strain (ε_y) in the longitudinal direction. In this paper, the stress-strain state is calculated on the basis of a nonlinear-viscous body model (model of plastic material with nonlinear hardening) describing creep curves, which are used to calculate the processes of shape change under conditions of super-plasticity. Figure 5 illustrates the distribution of dimensionless value of contact pressure (p). The values of force factors acting on the roller are equal to $\bar{P}_y = 4.1 \times 10^{-3}, \bar{P}_z = 0.011, \bar{M} = 3.4 \times 10^{-3}$.

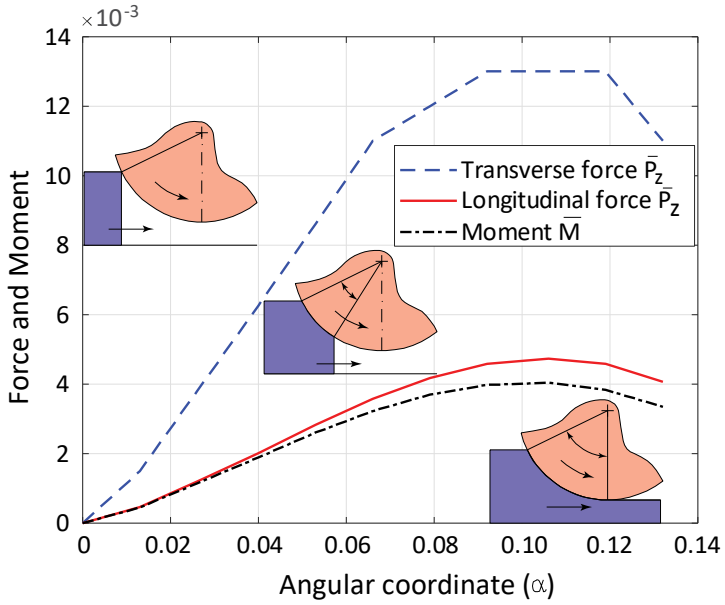

Fig. 6. Forces and moment acting on the roller

Figure 6 shows the graph of the change of dimensionless values of forces and the moment M depending on the contact angle. It can be established that there is an increase in the resistance from the material side to the roller at the beginning of the contact at its minimum angle and a significant decrease in the resistance at the end of the contact section. The dimensionless values of the moment and contact force change as the contact angle of the material with the roller increases. According to these graphs, it is possible to establish the values of force and moment of deformation and determine the required power of the technological equipment.

Calculations show that it is possible to select the friction coefficient μ and the length carrying ratio λ in such a way that the stress in the y-axis direction (σ_y) can be significantly reduced. At certain values of λ, the friction force q changes direction on a small section of the contact surface. The stress-strain state was calculated based on a nonlinear viscous body model. The nonlinear-viscous body model describes creep curves in the absence of the first section, i.e., when strain hardening is insignificant. At high temperatures, for all stresses and strain rates, there is usually no damped section in the creep curves. In the presence of linear initial sections in equation (2) it is necessary to put $\beta = 0$ and the creep curves will be described by the nonlinear-viscous body model, which is widely used for calculations of the processes of shape change under super-plasticity conditions.

3.1. ANALYSIS THE EFFECT OF LENGTH CARRYING RATIO

Figure 7 shows the dimensionless stress, contact pressure, force, and moments versus length carrying ratio (λ) diagrams. As λ increases, the longitudinal and transverse stresses decrease. In contrast, the equivalent stress does not change (Fig. 7a). On the other hand, the tendency for the contact pressure and the longitudinal, transverse forces and moment all increase when λ increases, as shown in Fig. 7b and Fig. 7c.

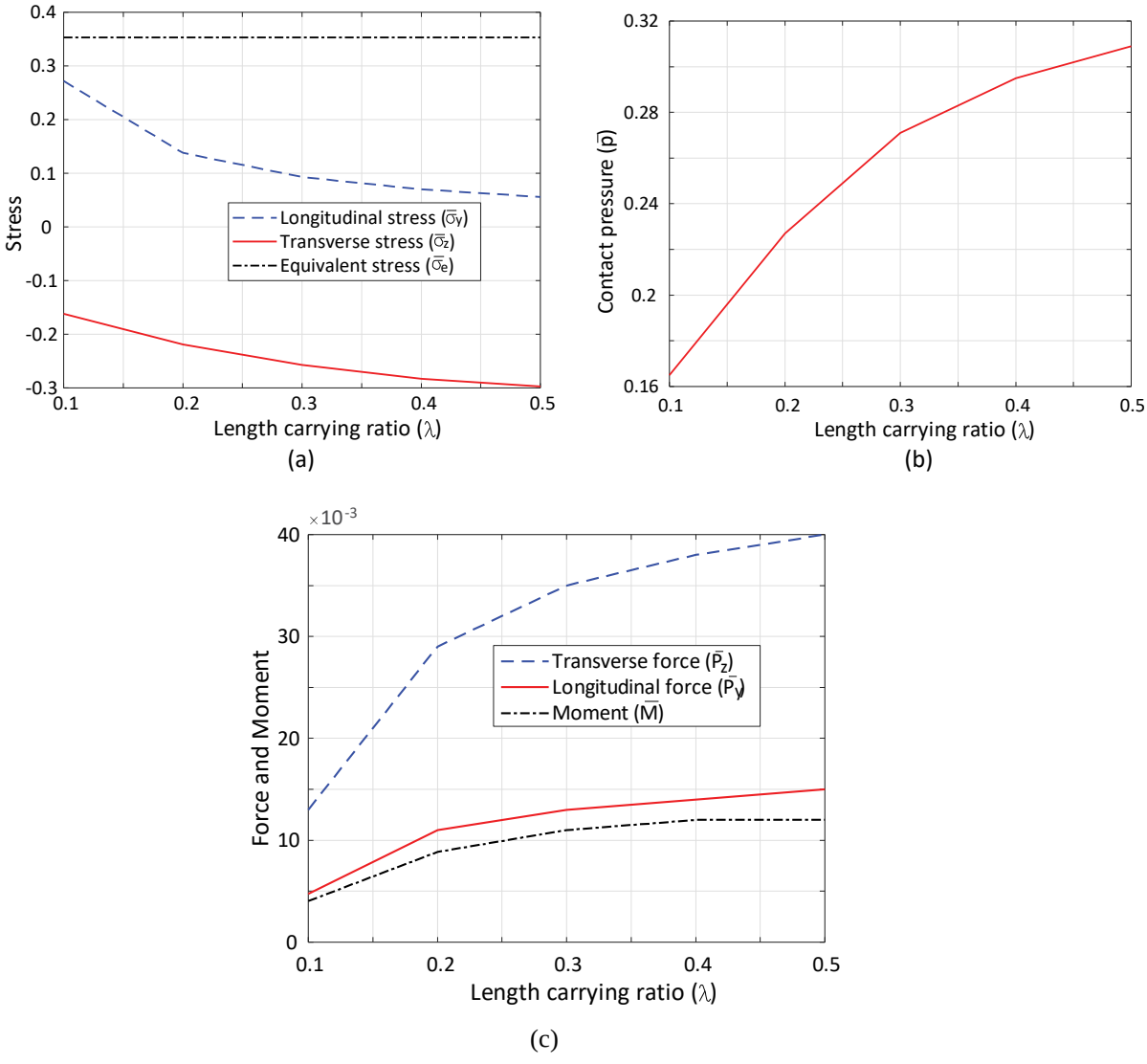

Fig. 7. The effect of dimensions ratio (λ)

It can be concluded that a decrease in the length carrying ratio (λ) leads to an increase in the roller radius and a change in the thickness of the surface layer. In general, this affects the recovery processes of the worn surface. The effect of λ on forces and torque indicates that using the bigger diameter roller can reduce the forces and torques and increase the efficiency of the restoration process.

3.2. ANALYSIS THE EFFECT OF FRICTION COEFFICIENT

Figure 8 shows the diagrams of dimensionless stress, contact pressure, force, and moments dependence on the friction coefficient (μ). With increasing μ, there is a gradual increase in longitudinal stress and a sharp increase in transverse stress, while the equivalent stress does not change (Fig. 8a). As the friction coefficient increases, the contact pressure and the transverse force decrease (Fig. 8b). However, the longitudinal force and moment are not heavily affected by the value of μ (Fig. 8c).

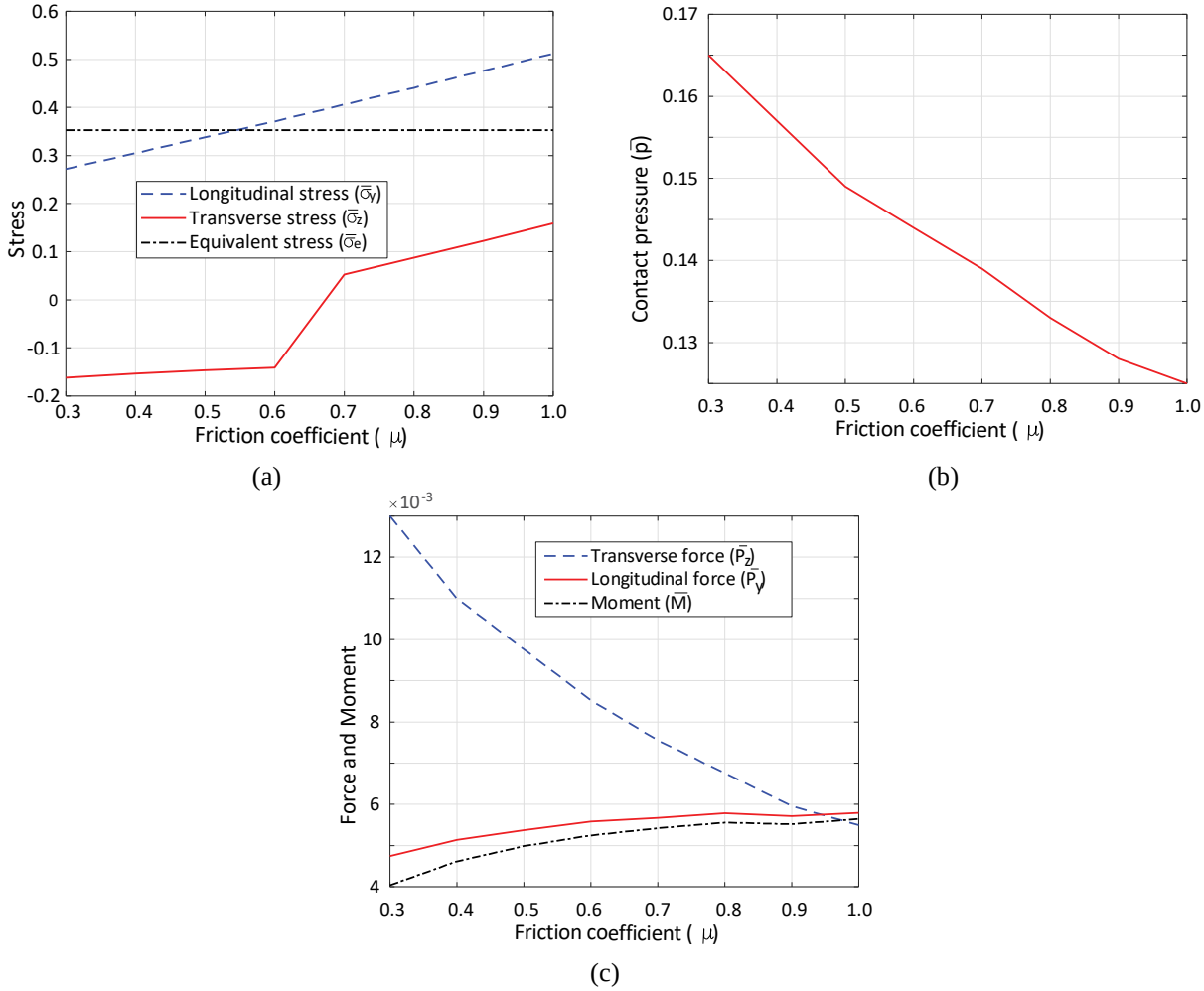

Fig. 8. The effect of friction coefficient (μ): $stress - a).$, $contact\ pressure - b)$, $force\ and\ moment - c)$

It is observed that the change in the friction coefficient (μ) on the contact surface of the material with the roller also affects the change in the values of forces and moments. At certain values, the friction forces change direction over a small contact surface area. The contact pressure takes the maximum value at the point of the contact surface with angular coordinate $\alpha = 0.05$ and then decreases. At values of $\lambda = 0.5$ and $\mu = 0.3$, the normal stress in the running-in direction decreases significantly and equals zero.

3.3. ANALYSIS THE EFFECT OF PROCESSING MATERIAL

Numerical calculations were carried out for the following values of material constants in the equation (3) $(m = 0.149; n = 0)$. Figure 9 shows the plots of stress components and equivalent stress in the deformation center when the different material is used.

Figure 10 shows the graph of pressure change on the roller. Comparing this scenario with the result of the hardening theory calculation in Fig. 5, it can be seen that the pressure decreases sharply to zero at the end of the contact section. The maximum value is reached at a much smaller contact angle than it is according to the hardening theory.

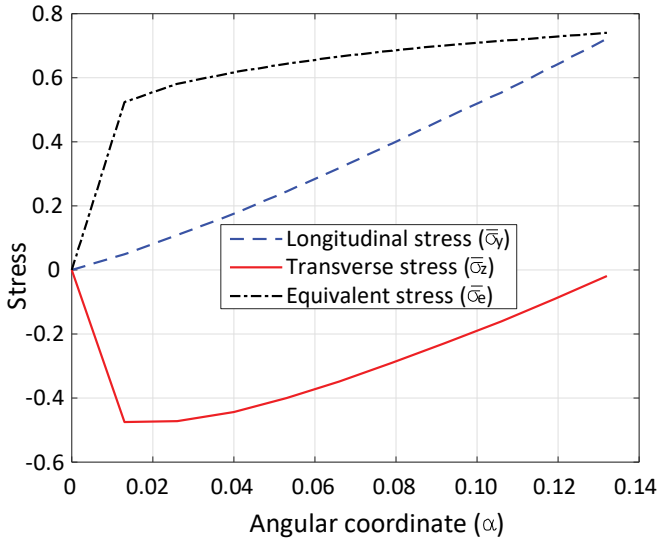

Fig. 9. Distribution of stress components and equivalent stress in the deformation center for nonlinear viscous material $(m = 0.149; n = 0)$

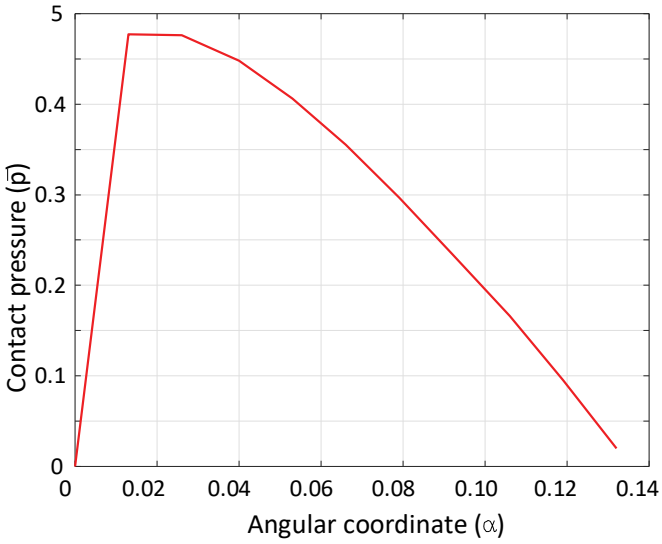

Fig. 10. Distribution of contact pressure on the roller for nonlinear viscous material $(m = 0{,}149; n = 0)$

The main resistance from the side of the material to the roller comes at the beginning of contact, and then sharply decreases. A similar pattern is observed for the force parameters of the technological process, presented in Fig. 11, if we compare them with the results of the hardening theory calculation (Fig. 6).

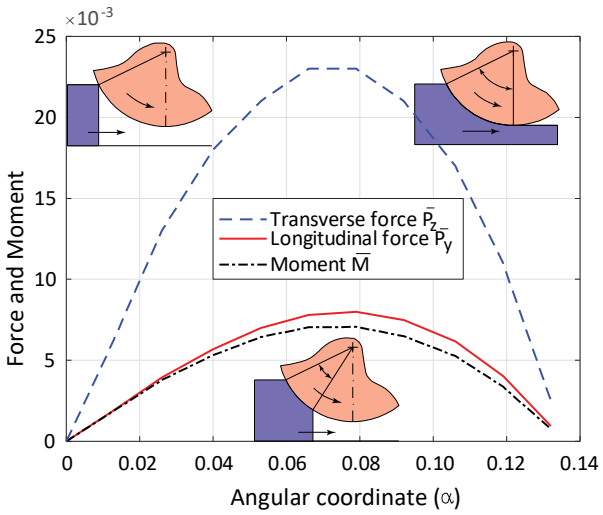

Fig. 11. Forces and moment acting on the roller for nonlinear viscous material ($m = 0{,}149; n = 0$)

4. CONCLUSIONS

The paper calculates the stress-strain state based on a nonlinear viscous body model describing creep curves, which are used to calculate shape change processes under superplasticity conditions. In formulating the one-dimensional problem of inelastic deformation of the clad layer during roller rolling, relatively general formulas for calculating the force parameters of the technological process were obtained. By calculations, using the application program in the mathematical editor Mathcad for numerical analysis of the nonlinear one-dimensional problem, it is observed that (1) the stress-strain state in the deformation zone depends significantly on the thickness of the layer before deformation, the radius of the roller and the friction coefficient on the contact surface between the material and the roller, and (2) at their certain values, the friction forces change direction on a small section of the contact surface. The contact pressure takes the maximum value at the point of the contact surface with angular coordinate $\alpha = 0{,}05$ and then decreases. At values $\lambda = 0.5$ and $\mu = 0.3$, the normal stress in the running-in direction decreases significantly and equals zero. The dimensionless values of the moment and contact force change as the contact angles of the material with the roller increase. The results of the research and analysis are significant for establishing the mode of thermomechanical treatment and the selection of technological equipment for the restoration of flat surfaces of parts by rolling.

ACKNOWLEDGEMENTS

This research was funded by the Science Committee of the Ministry of Science and Higher Education of the Republic of Kazakhstan under the project grant number AP19680395 "Study of the stress-strain state of deposited parts and development of a method for reducing their deformations in the processes of surface plastic deformation".

REFERENCES

[1] KIPIANI P.N., ZIVZIVADZE L.I., SHALAMBERIDZE M.Sh., 2012, *The Influence of Surfacing Modes on the Resistance of Metal Against the Formation of Hot Cracks When Surfacing Ridges and Bands of Locomotive Wheels*, Tr. KSTU, 2/12, Kutaisi, 162–167.

[2] KIPIANI P.N., KOTLYAROV A.N., 1998, *The Influence of Technological Factors on the Quality of Deposited Metal During the Restoration of Wagon Wheel Ridges*, Collection of Scientific Papers, Resource-Saving Technologies for the Restoration of Railway Equipment by Welding, Surfacing and Spraying, Moscow, 46–51.

[3] KASRADZE D.Kh., GACHECHILADZE G.R., KASRADZE T.D., 2001, *Types of Thermomechanical Reflow (TMR) of Clad Surfaces*, International Scientific Journal, Problems of Applied Mechanics, 4/5.

[4] BOIKO N.I., KHACHKINAIAN A.E., 2003, *Improvement of the Structure of the Clad Metal of Parts by Surface Plastic Deformation*, Proc. 62nd University Scientific-Theoretical Conf. of Prof.-Prep. Soc., Transport-2003, Rostov-n/D, RSUPS, 161–162.

[5] BOYKO N.I., KHACHKINAIAN A.E., 2003, *Mathematical and Computer Modeling of the Technological Process of the Surface Plastic Deformation of the Clad Layer of the Parts. Actual Problems of Railway Transport Development*, Collection of Scientific Articles of Young Scientists, Graduate Students and Doctoral Students. Edited by Dr. of Technical Sciences, Prof. A.N. Guda – Rostov-N/D: Rostov State University of Railway Transport, 21–24.

[6] TONYSHEVA O.A., VOZNESENSKAYA N.M., SHALKEVICH A.B., 2012, *Investigation of the Influence of High-Temperature Thermomechanical Processing on Structures, Technological, Thermal and Mechanical Properties of High-Temperature Thermomechanical Treatment on Structures, Technological, Mechanical and Corrosion-Resistant Properties of High-Alloyed Corrosion-Resistant Steels with Increased Nitrogen Content*, Aviation Materials and Technologies, 3, 31–36.

[7] KASRADZE D.Kh., GACHECHILADZE G.R., KASRADZE T.D., 2001, *Types of Thermomechanical Backflow (TMF) of Clad Surfaces*, International Scientific Journal, Problems of Applied Mechanics, 4/5.

[8] SHVEIKIN V.P., FEDOROVA A.A., 2014, *Main Parameters of High-Temperature Thermomechanical Processing Affecting the Properties of Rolled Products*, International Conference, Innovative Technologies in Metallurgy and Mechanical Engineering, Yekaterinburg, 159–164.

[9] SERGEEV N.N., SERGEEV A.N., KUTEPOV S.N., GVOZDEV A.E., AGEEV E.V., 2019, *Influence of Operating Modes of High-Temperature Thermomechanical Processing on Mechanical Properties of Reinforcing Bars*, Proceedings of the Southwest State University, 23/2, 29–52, (in Russian), https://doi.org/10.21869/2223-1560-2019-23-2-29-52.

[10] KARAMYSHEV A.P., et al., 2016, *Investigation of Strain Hardening and Damage of Billets from Heavy Tungsten-Based Alloys*, International Scientific and Technical Conference, Nano-technology of Functional Materials (NFM 16), Sankt-Petersburg, June 21–25, 148–154.

[11] UDALOV A.A, PARSHIN S.V, UDALOV A.V, VASILEVYKH S.L, 2019, *Power Parameters of the Process of Hardening of Cylindrical Parts by a Toroidal Roller by the Method of Surface Plastic Deformation*, IOP Conf. Series: Journal of Physics, 1210, 012150, https://doi.org/10.1088/1742-6596/1210/1/012150.

[12] BULEKBAEVA G.Zh., KIKVIDZE O.G., KIPIANI P.N., MINDADZE S.O., 2016, *Plastic Deformation as a Means to Eliminate Defects Such as Cracks in Welded Joints*, Kutaisi, Bulletin of Akaki Tsereteli State University, 1/7, 45–60.

[13] KIKVIDZE O.G., BULEKBAEVA G.Zh., KIPIANI P.N., 2016, *Plastic Deformation of the Deposited Layer on a Flat Surface*, Georgian Engineering News, 1/77, 64–66.

[14] KIPIANI P.N., MINDADZE S.O., BULEKBAEVA G.Zh., 2015, *Energy-Saving Technologies with the Use of Plastic Deformation After Cooking During Welding and Surfacing of High-Strength Steels*, International Scientific Conf.: Energy - Regional Problems and Development Prospects, 24–25 Oct. 2015, Kutaisi, 234–236.

[15] BULEKBAYEVA G., BRZHANOV R.T., 2020, *Rolling of a Weld Pad on a Flat Surface. One-dimensional problem, IOP Conference Series: Materials Science and Engineering.* IOP Publishing, 962, 022053, https://doi:10.1088/1757-899X/962/2/022053.

[16] BULEKBAEVA G., KIKVIDZE O.G., LAKHNO V., BRZHANOV R., TABYLOV A. SMIRNOV S., 2019, *Computer Simulation in the Mathcad Package of Plastic Deformation of the Deposited Layer on the Flat Surface of the Part,* Journal of Theoretical and Applied Information Technology, 97/20, 2467–2484.

[17] PAPYRIN A.N. KLINKOV, S.V., KOSAREV V.F., 2004, *Modeling of Particle-Substrate Adhesive Interaction Under the Cold Spray Process*, itsc2003p0027, 27–35, https://doi.org/10.31399/asm.cp.itsc2003p0027.

[18] KASRADZE D.H., 2001, *Calculation of Deformation Resistance During Thermomechanical Treatment (TMO) of Deposited Surfaces for a Two-Dimensional Deformation Zone*, International Scientific Journal, Problems of Applied Mechanics, 4/5.

[19] HEIGEl J.C., MICHALERIS P., REUTZEL E.W., 2015, *Thermo-Mechanical Model Development and Validation of Directed Energy Deposition Additive Manufacturing of Ti–6Al–4V,* Additive Manufacturing, 5, 9–19. https://doi.org/10.1016/j.addma.2014.10.003

[20] KIKVIDZE O.G., et al., 2011, *Calculation of the Boundary Layer During Plastic Deformation of Surfaces,* Engineering News of Georgia, 60/4, 51–55.